$\Omega_{\rm B}$ and Ω_0 From MACHOs and Local Group Dynamics

G. Steigman[1] and I. Tkachev[1,2,3]

[1] *Departments of Physics & Astronomy, The Ohio State University Columbus, OH 43210*

[2] *Institute for Nuclear Research of the Academy of Sciences of Russia Moscow 117312, Russia*

[3] *TH Division, CERN, CH-1211 Geneva 23, Switzerland* [4]

ABSTRACT

We obtain restrictions on the universal baryon fraction, $f_{\rm B} \equiv \Omega_{\rm B}/\Omega_0$, by assuming that the observed microlensing events towards the Large Magellanic Cloud are due to *baryonic* MACHOs in the halo of the Galaxy and by extracting a bound to the total mass of the Milky Way from the motion of tracer galaxies in the Local Group. We find a lower bound $f_{\rm B} > 0.29^{+0.18}_{-0.15}$. Consistency with the predictions of primordial nucleosynthesis leads to the further constraint on the total mass density, $\Omega_0 \lesssim 0.2$.

Subject headings: MACHO — dark matter — Local Group

[4] Current address

1. Introduction

It is a Herculean task to inventory the contents of the Universe (e.g., Fukugita, Hogan, & Peebles 1997). A more modest goal might be to pin down the baryonic fraction of the total mass, $f_{\rm B}$ (e.g., White et al. 1993, Steigman & Felten 1995). If objects can be identified which are likely to provide a "fair" sample of $f_{\rm B}$, we may avoid the daunting prospect of having to identify all the guises baryons may assume. Large clusters of galaxies offer a very promising site (White et al. 1993; Steigman & Felten 1995; Evrard 1997; Steigman, Hata & Felten 1997). To test the estimates of the systematic errors in $f_{\rm B}$ derived from X-ray cluster data, it would be of value to measure $f_{\rm B}$ in a completely different system, provided a case could be made that it will provide a "fair" sample. Suppose, for example, we could estimate the baryonic mass associated with the Galaxy. If we could also measure the corresponding "dynamical" mass, we could obtain an independent estimate of $f_{\rm B}$ whose systematic uncertainties (and dependence on the Hubble parameter) differ from those which accompany the X-ray cluster determinations. In this paper we focus on the Local Group of galaxies (LG), using the MACHO mass estimates (Alcock et al. 1997a) for a lower bound on the baryonic mass and relying on LG dynamics to constrain the total mass estimate.

Microlensing experiments (Alcock et al. 1997a) suggest that roughly half the mass in the halo of our Galaxy, out to the distance of the Large Magellanic Cloud (LMC), may be in the form of Massive Compact Halo Objects (MACHOs). One can imagine several exotic possibilities for the nature of the MACHOs. They could be very dense clusters of non-baryonic dark matter with special properties that allow them to clump inside their Einstein ring radii (Kolb & Tkachev 1994), or they could be primordial black holes. Neither of these possibilities is especially well motivated and each has its intrinsic difficulties, but neither can be excluded a priori. Stellar remnants such as old white dwarfs[1] appear to offer a more natural candidate (Alcock et al. 1997a) which, however, is not without its problems too [e.g., white dwarfs require a rather narrow initial mass function in order to avoid overproducing low-mass stars or supernovae (Adams & Laughlin 1996)]. Dense and cold baryonic gas clouds have also been considered as a viable alternative for the observed gravitational microlenses (Henriksen & Widrow 1995; Gerhard & Silk 1996). Finally, it must be kept in mind that the observed microlensing may be due to objects which are not in the halo of the Galaxy. If the MACHOs are, indeed, stellar remnants (or cold baryonic gas clouds) in the halo of the Galaxy, then the mass of baryons within 50 kpc of the Galactic center is $M_{\rm B}(50\ {\rm kpc}) \geq M_{\rm MACHO} = 2.0^{+1.2}_{-0.7} \times 10^{11} M_\odot$ (Alcock et al. 1997a).

The purpose of the present paper is to extract information on the universal baryon fraction from this number assuming the MACHOs are revealing baryonic matter in the Galaxy halo, and from the dynamics of the Local Group of galaxies. The constraint we obtain may be compared to the one derived from X-ray galaxy clusters (see, e.g., Steigman & Felten 1995; Evrard 1997; Steigman, Hata & Felten 1997), but it relies on different observations in a completely different physical system on a vastly different scale and, interestingly, has a different dependence on the Hubble parameter ($H_0 \equiv 100h$ km s^{-1} Mpc^{-1}).

The value of $M_{\rm B}(50\ {\rm kpc})$ derived from microlensing experiments is approximately 50% of the total mass of the Galaxy out to this distance. The latter mass, presumably the sum of baryons and cold dark matter, is derived dynamically (see, e.g., Kochanek 1995). However, on the basis of this we cannot conclude that the primordial baryon fraction is $f_{\rm B} \approx 0.5$. Baryons are "strongly" interacting particles, while for the (non-baryonic) cold dark matter all interactions except gravitational can be neglected. Consequently, the density profile of the baryonic matter does not necessarily follow the density profile of the cold dark matter, and baryonic matter may be more (or less) concentrated towards the center of the gravitational well. However, we may be able to estimate the primordial baryon fraction if we take the ratio of baryons (as revealed by the MACHOs) to the total mass on some larger scale, which should be sufficiently large so that the matter inflow or outflow across the boundary of the region is negligible.

The total mass of matter residing in such a larger region can be found dynamically; however, we cannot measure the mass of baryons separately on such larger scales. Although the baryonic halo may be expected to extend outside of the 50 kpc scale (in the form, e.g., of MACHOs, diffuse gas, satellite Galaxies, etc.), by neglecting these extended baryons we can obtain a lower bound on $f_{\rm B}$. Indeed, while in the past there might have been violent processes of baryon ejection from the Galaxy accompanying, e.g., supernova explosions, analogous ejecta of cold

[1] Neutron stars and black holes of stellar origin cannot constitute a significant halo fraction in view of the constraints arising from the observed metallicity and helium abundances (Ryu, Olive & Silk 1990).

dark matter is not expected. Therefore, by neglecting the unknown ejected component of baryons we will be on the "safe side" in our inequality for $f_{\rm B}$, which, we emphasize, does rely on our assumption that MACHOs are baryonic matter in the halo of the Galaxy.

For the larger reference scale we can choose the current turnaround radius for the LG. Initially, every shell of the Galaxy's building material expands with the Universe. Gradually, this expansion slows down and eventually a gravitationally bound shell separates from the general expansion. This shell stops expanding and then collapses (Gunn & Gott 1972). The radius of this first stopping point is the turnaround radius. With the passage of time shells that are more and more distant and less and less bound turn around sequentially, i.e., the turnaround radius propagates outward with time (for details see, e.g., Filmore & Goldreich 1984; Bertschinger 1985; Sikivie, Tkachev & Yun Wang 1995, 1997). There is one shell that is turning around now, at present; the corresponding distance of this shell from the center of mass of the system is the current turnaround radius. Collisionless cold (non-baryonic) dark matter is restricted to remain within this radius, which is just what we want for the larger reference scale. This picture of infall is valid independent of the assumption of spherical symmetry (the turnaround sphere will become a turnaround surface); for the model to be tractable analytically, we do assume spherical infall.

2. Spherical Infall Model

Let R be the current turnaround radius, $M_{\rm B}(R)$ the mass of all baryons currently inside this radius, and $M_{\rm tot}(R)$ the total mass within R. We are using the ratio $M_{\rm B}(R)/M_{\rm tot}(R) = f_{\rm B}$ to provide a measure of the universal baryon fraction, $f_{\rm B} = \rho_{\rm B}/\rho_{\rm tot} = \Omega_{\rm B}/\Omega_0$. For $R \geq 50$ kpc, we expect $M_{\rm B}(R) \geq M_{\rm B}(50\ {\rm kpc})$. Furthermore, there may be more baryons that were initially associated with the Galaxy than those that are currently within 50 kpc. As a consequence, our estimate provides a *lower* bound on the universal fraction of baryons: $f_{\rm B} > M_{\rm B}(50\ {\rm kpc})/M_{\rm tot}(R)$.

Actually, in computing this inequality we do not have to use the current turnaround radius. It is equally legitimate, and will provide a tighter constraint, to take any smaller radius that satisfies the following condition: matter which is falling freely and is currently at this radius has not yet had a chance to cross previously collapsed material. In other words the shell is outside the first caustic of the spherical infall model. The position of the first caustic is model dependent, but it has its largest value relative to the turnaround radius if the initial overdensity causing the infall can be considered as a point mass excess. Let us denote the radius of the first caustic as R_1 and the total mass inside of it as M_1. In the point mass excess case (and for $\Omega_0 = 1$), $R_1 = 0.37R$ and $M_1 = 0.7M(R)$, (Sikivie, Tkachev & Yun Wang 1997).

Before shell crossing the radius of any given shell obeys the equation of motion

$$\frac{1}{2}\dot{r}^2 - \frac{GM}{r} = -E\ , \tag{1}$$

where M is the mass interior to the shell and E is its binding energy per unit mass; both are constants prior to shell crossing. Solutions can be parameterized as

$$\begin{aligned} r &= A(1-\cos\theta)\,, \\ t &= B(\theta - \sin\theta)\,, \end{aligned} \tag{2}$$

where $A \equiv GM/2E$, $B \equiv GM/(2E)^{3/2}$.

Small galaxies in the Local Group that are close to the turnaround sphere can be considered as tracers of the motion of the corresponding shell. If the distances to such galaxies and their radial velocities are known at time t, we can write, according to equations (2):

$$\frac{vt}{r} = \frac{\sin\theta(\theta-\sin\theta)}{(1-\cos\theta)^2}\,, \tag{3}$$

$$M = \frac{v^2 r}{G(1+\cos\theta)}\,. \tag{4}$$

Using equation (3) we can solve for θ which is then used in equation (4) to determine the total mass M interior to the shell on which the tracer galaxy resides. Note that the derivation of the relation $M = M(r, v, t)$ does not rely upon the initial mass distribution (in other words we do not need to know the function $E = E(r_0)$). In the spherical infall approximation M gives a direct "weighing" of the LG at each radius where a known satellite galaxy resides. We shall use this procedure for a subset of galaxies that are close to the turnaround surface.

On the other hand, suppose that the initial mass distribution for unperturbed Hubble flow is known, e.g., $M(r_0) = 4\pi\rho r_0^3/3 + \delta M(r_0)$, where $\delta M(r_0)$ is an (initially small) excess mass over homogeneous cosmological background. A good example corresponds to the assumption of all excess mass concentrated at the origin, $r_0 = 0$ (point mass excess). Using the integrals of the equations of motion written as $M(r, v, t) = M(r_0(r))$, we can find the velocity field at any given point, $v = v(r, t)$. The trajectory in the $\{r,\, v\}$ phase space, $v = v(r)$, representing

occupied cells at a given moment of time is called the infall trajectory. For example, if the initial overdensity is scale independent, $\delta M/M = (M_0/M)^\epsilon$, and for $\Omega = 1$, the infall trajectory is given by

$$r = R(\frac{1-\cos\theta}{2})\left(\frac{\pi}{\theta-\sin\theta}\right)^{2/3+2/9\epsilon}, \quad (5)$$

$$v = \frac{r}{t}\frac{\sin\theta(\theta-\sin\theta)}{(1-\cos\theta)^2}, \quad (6)$$

The point mass excess case corresponds to $\epsilon = 1$.

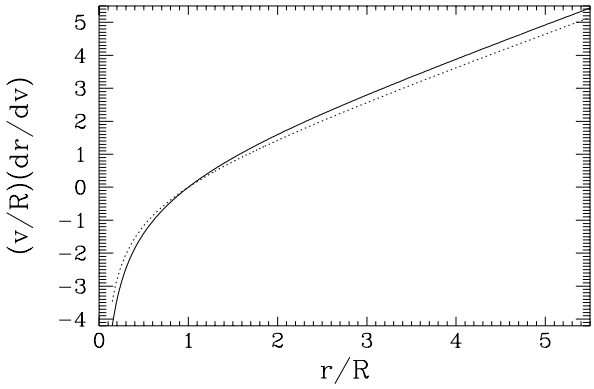

Fig. 1.— Infall trajectories for the cases $\Omega = 1$ (solid line) and $\Omega \to 0$ (dotted line).

In the case $\Omega < 1$ the analytical expressions which give an infall trajectory are more complicated and we do not present them here. It is important, however, that at large r the overdensity can be neglected and all infall trajectories tend to the simple Hubble law, $v = Hr$. It is convenient to choose as physical parameters which characterize an infall trajectory the turnaround radius, R, and the Hubble constant, h, which is the slope of $v(r)$ at $r \gg R$. When R and h are are fixed, the infall trajectories that correspond to different cosmological models, or different excess mass profiles, differ insignificantly outside of the first caustic. For comparison we plot infall trajectories for the case $\Omega = 1$, $\epsilon = 1$ and $\Omega \to 0$, $\epsilon = 1$ in Fig. 1. The difference between the two cases is significantly smaller than the uncertainties in the measured galaxy peculiar velocities (see below). Either trajectory from Fig. 1 can be used in fitting the data to determine R and h. For definiteness in our fitting procedure, we use the infall trajectory which corresponds to $\Omega = 1$ and assume its validity for the general cosmological model (if, instead, we had used the $\Omega \to 0$ trajectory, the change in R would have been $\approx 3\%$). To avoid confusion, note that in this approach Eq. (6) cannot be used to find $h = h(t)$ (this equation gives $H = 2/3t$, as it should for $\Omega = 1$), but $h = h(t)$ has to be taken to match the underlying cosmology.

In applying spherical infall to the Local Group there is a complication. Interior to the turnaround surface there are two large galaxies of roughly equal mass: the Milky Way and Andromeda (M31), M31 being somewhat larger. In what follows we adopt, following Peebles (1996), for the ratio of their masses, $M_{\rm MW} = 0.7M_{\rm A}$. The derived mass and the turnaround radius of the LG will be a consequence of the gravitational pull of both galaxies. We assume that those tracer galaxies that are sufficiently far away are infalling to the common center of mass of the Milky Way/M31 system.

We utilize χ^2 modeling of the infall trajectory, Eq. (6), for the whole sample of galaxies in the local volume (excluding those satellites close to the Milky Way and Andromeda). This may result in a more statistically robust determination of R compared to the direct "weighing" at some selected positions through the use of equations (3) and (4).

In the spherical infall modeling of the Local Group defined in this way, M31 is used only to determine the LG center of mass and does not appear explicitly on the infall diagram. However, in the description of the M31/MW system another approximation can be made, namely that of two, isolated, mutually gravitating, compact bodies. Using this approximation, the total mass of the system can be derived. This is the so-called "timing argument" of Kahn & Woltjer (1959).

3. M31 timing

Let us assume that, at present, the relative motion of the Galaxy and M31 can be described as motion of two, mutually gravitating, compact bodies with masses m_1 and m_2. The conserved total energy of the system is

$$E_{\rm tot} = \frac{m_1 m_2}{m_1+m_2}\left[\frac{1}{2}V^2 - \frac{GM}{d}\right], \quad (7)$$

where $M \equiv m_1 + m_2$, V is velocity of M31 as seen from the Galaxy, and d is the distance between them. This gives the equation of motion which is identical to Eq. (1) but with E being replaced by $\tilde{E} \equiv E_{\rm tot}M/m_1m_2$. Since $\tilde{E}$ is unknown (as is E), this variable can be replaced by another variable, t, using solutions, Eqs. (2). In this way Eqs. (3) - (4) are reproduced with the coordinates relative to the center of mass, r, v, being replaced by coordinates relative to the Galaxy, d, V, and M is the total mass of the MW/M31 system. Using the observed values of d, V, and t, $M = M(d, V, t)$ can be calculated.

As we shall see, the mass calculated in this way exceeds the predictions of the spherical infall by about a factor of two. This is a serious internal contradiction in our modeling of LG dynamics and it has to be addressed.

There are several caveats in the M31 timing argument. $\tilde{E}$ can be related to t only if the equation of motion, Eq. (7), is valid at all times. But this is not generally true. The dominant galaxies started to grow from small initial fluctuations which were *extended* in space. Their masses were not constant, but grew because of infall and the merging of smaller, progenitor galaxies.[2] The "timing" approach can be modified assuming that $m_i = m_i(t)$, with the growth rate taken from the spherical infall model for each galaxy halo separately, and assuming that the resulting motion of galaxies can be described as the motion of point particles on an unperturbed cosmological background. However, there is a caveat to this approach too. The background cannot be considered as unperturbed, especially at those late stages when large extended halos grow at the expense of surrounding material.

The accuracy of the timing argument with respect to the neglect of finite size effects can be tested using the results presented by Peebles et al. (1989), where LG formation was modeled using N-body simulations. The results of Peebles et al. (1989) can be considered as a generalization of M31 timing which accounts for the finite sizes and for the finite perturbations of the cosmological background. Results were presented there for two values of the present age, $t = 7.8$ Gyr and $t = 13.8$ Gyr. For $t = 7.8$ Gyr, the mass of the Milky Way/M31 system derived from the timing argument was $7.6 \times 10^{12} M_\odot$, while the LG mass inside the turnaround surface measured in the N-body experiment was $4.9 \times 10^{12} M_\odot$. For $t = 13.8$ Gyr, the timing argument gives $4.6 \times 10^{12} M_\odot$, while the mass inside the turnaround surface was found to be $3.5 \times 10^{12} M_\odot$ in the N-body simulation. The agreement is not very good, with M31 timing overestimating the mass inside the turnaround surface. The calculations of Peebles et al. (1989) were restricted to an $\Omega_0 = 1$ universe; we are unaware of analogous results for an open universe model. In contrast, the predictions of the spherical infall model are valid irrespective of the value of Ω_0.

Last but not least, from our point of view the most serious drawback of the M31 timing is that it uses a single observation. Since unknown peculiar velocities are inevitably present in the motion of any galaxy, the results derived from just one data point can deviate significantly from the mean. In contrast, when the motion of a large set of "test particles" is considered, which can be done in spherical infall modeling, the peculiar velocities may average out. For this reason we prefer the spherical infall approach to the M31 timing argument. Unfortunately, not many galaxies are available for modeling the motion near the turnaround surface and it would be inappropriate to ignore the information provided by the motion of M31. For these reasons we adopt the following procedure.

We assume that all galaxies belonging to the Local Group have started in a common initial environment. Therefore, we can try to relate $\tilde{E}$ in Eq. (7) to E which enters the equation of motion for the other, outlying satellites of the Local Group, Eq. (1). (Each satellite has its own value of E, determined by its initial position.) In this way it is possible to put M31 on the infall diagram along with the rest of the galaxies. Assuming two initial small overdensities (one the seed of the Galaxy, the other the seed of M31) on an otherwise unperturbed initial Hubble flow, we find that the data points (r,v), where r and v are the distance and velocity of the Local Group satellites as seen from the center of mass, along with the data point (d,V), corresponding to M31 as measured from the Galaxy, all belong to one and the same infall trajectory to a very good approximation. This procedure, which would overestimate the mass of the Local Group if there were an extra mass excess (say, unseen matter residing in the center of mass), will be our basic approach to bounding mass of the Local Group from above.

4. Infall in the Local Group.

Our basic assumption is that those tracer galaxies sufficiently far away are infalling to the common center of mass of the MW/M31 system. In addition, we have to make an assumption about the relative velocity of the Milky Way. We assume that, relative to the sample of sufficiently close galaxies, $r < D$, the Milky Way also infalls to the common center of mass. However, the Local Group as a whole may be moving with respect to the more distant galaxies. To account for this possible local deviation from the Hubble flow, we determine from our fitting procedure the Milky Way velocity relative to the sample of galaxies at $r > D$, as well as the distance D itself. We utilize the χ^2 approach to modeling the infall

[2]These objections do not apply to the spherical infall model as long as spherical symmetry holds.

trajectory; i.e. we look for the minimum of the sum

$$\sum_i \left[v(i) + \vec{v}_{\rm MW} \cdot \vec{e}(i) - v(r)\, \vec{e}_{\rm cm} \cdot \vec{e}(i)\right]^2 \ , \qquad (8)$$

where $v(i)$ is the measured velocity of i-th galaxy, $\vec{e}(i)$ is the unit vector pointing from the center of mass to the direction of that galaxy, $\vec{e}_{\rm cm}$ is the unit vector pointing from the Galaxy to the center of mass (i.e., according to our assumption, in the direction of M31), $v(r)$ is the infall trajectory, Eqs. (5), (6), and $\vec{v}_{\rm MW}$ is the Milky Way velocity. Relative to a set of galaxies with $r(i) < D$, the Milky Way velocity is assumed to be $v_{\rm MW} = v_{\rm M31}(1 + M_{\rm MW}/M_{\rm M31})^{-1}$. M31 itself is included in this fit, as explained in the previous Section. We do this modeling in §4.1. For comparison, in §4.2, we apply equations (3) - (4) for the direct "weighing" of the Local Group, using the subset of galaxies which lie closest to the turnaround sphere.

We don't expect the spherical approximation to be accurate for nearby galaxies with distances from the center of mass of the LG comparable to their distances from one of the dominant galaxies. We exclude from the fit Eq. (8) the close satellites of either the Milky Way or M31. On the other hand, radial infall in the direction of one of the dominant galaxies may be a good approximation for close satellites (so that the satellite does not "feel" the other heavy galaxy). Most such satellites are inside the first caustic of the infall model, where their trajectories are very model dependent. Luckily, there are two satellites that might be just outside the first caustic. Using Eq. (4), in §4.3 we derive the mass interior to these satellite galaxies under the assumption of radial infall to one of the dominant galaxies.

4.1. Modeling the infall trajectory.

We included in our fit to Eq. (8) all galaxies in Karachentsev & Makarov (1996) at distances less than 3 Mpc from the center of mass of the Milky Way/M31 system; we excluded those whose distances from either the Milky Way or M31 are smaller than 0.3 Mpc. The resulting best fit trajectory, as well as the data points recalculated relative to the center of mass are shown in Fig. 2. Data points are connected by the dotted line in order of increasing r; the first ten galaxies are listed in Table I.

The parameters of the best fit trajectory are: $R = 0.93$ Mpc, $h = 0.69$ and $D = 1.5$ Mpc. The formal $\Delta\chi^2 = 2.3$ confidence contour in the R, h plane is shown by the solid line in Fig. 3. After we had completed the analysis presented here a new data set compiled by Mateo (1998) became available. According to Mateo, the distance of Leo A, the "low" velocity point at $r = 1.6$ Mpc in Fig. 2 (see also Fig. A8), should be smaller by a factor of two, placing it right on our best fit trajectory. We have repeated the analysis described here using Mateo's data, finding $R = 0.9$ Mpc and $h = 0.6$.

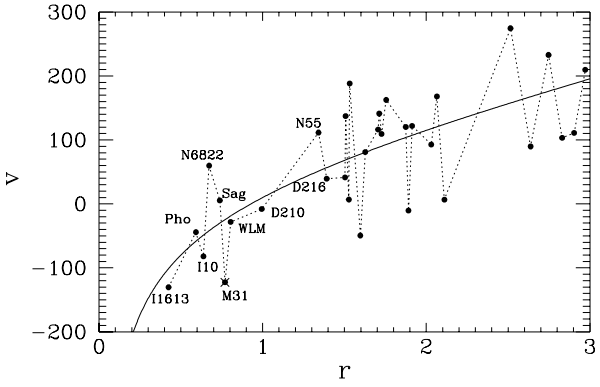

Fig. 2.— Phase space for the sample of nearby galaxies deriveded under the assumption of infall to the center of mass of the Milky Way – M31 system. The distance (r) from the center of mass is in Mpc, the infall velocity (v) is in km/s. For M31, r and v are the distance and the velocity relative to the Galaxy. The best fit infall trajectory, corresponding to $R = 0.93$ Mpc and $h = 0.69$, is shown by the solid line.

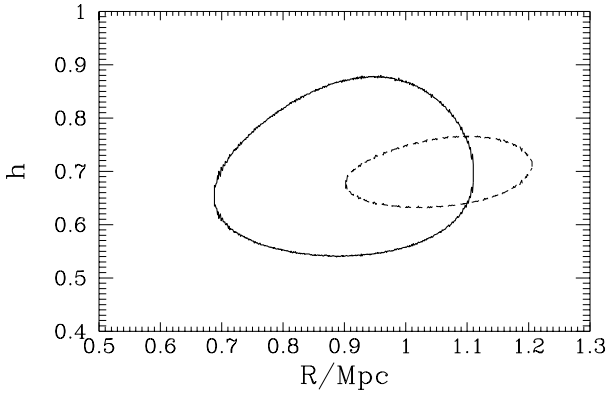

Fig. 3.— The $\Delta\chi^2 = 2.3$ confidence contour in the Hubble parameter (h) – LG turnaround radius (R) plane is shown by the solid line. The dotted line corresponds to the case when galaxies forming subclusters were removed from the fit; see the Appendix for details.

It was assumed that, with respect to galaxies in the volume whose scale is $r < D$, the Milky Way infalls to the common center of mass, while we fitted the Galaxy velocity with respect to galaxies in the volume $D < r < 3$

Mpc. This allows us to take into account the possible motion of the Local Group as a whole. If we were to neglect the Local Group velocity, i.e., if $D = \infty$ were assumed, the turnaround radius would be smaller, the value of the Hubble constant would be larger, and the velocity dispersion would increase. Our fit is made using the value of the Milky Way velocity found with respect to the whole set of galaxies in this volume, not with the velocity being allowed to vary with r. It is, however, instructive to study the trend of the Milky Way velocity derived with respect to the galaxies in volumes of varying depth. In this way we can test the self-consistency of the assumption of infall to the center of mass of the Milky Way/M31 system in the volume $r < D = 1.5$ Mpc. We defer a discussion of this trend to Appendix A.

We may conclude that $r = D \approx 1.5$ Mpc is a boundary of the Local Group. Note that despite the possibility that many galaxies in the sample at $r > D$ may be forming gravitationally bound groups of their own, which would induce additional peculiar velocities, the velocity dispersion turns out to be very small, $\sigma_v = 67$ km s^{-1} (using Mateo's (1998) data set, $\sigma_v = 50$ km s^{-1}). This value, which is significantly smaller than what might be expected in the standard ($\Omega_0 = 1$) CDM, $\sigma_v \sim 500$ km s^{-1} (Gelb & Bertschinger 1994), may be a signature of low density ($\Omega_0 < 1$).

Pairwise velocities of gravitationally bound pairs of galaxies or, more generally, the local infall and virialized components of velocites of galaxies which form remote clusters, make significant contributions to this velocity dispersion. One might expect that the picture of infall onto the Local Group will be "cleaner" if close pairs of galaxies are removed and only relatively isolated galaxies are selected for the fit. This procedure and the results are discussed in Appendix A. The resulting confidence contour in the R, h plane is shown by the dashed line in Fig. 3; the best fit values are: $R = 1.07$ Mpc, $h = 0.71$. The best fit turnaround radius obtained when all galaxies are included is $R = 0.93$ Mpc; in the case when subclusters were removed, $R = 1.07$ Mpc. These are within "1 σ" of each other. While the procedure with the subclusters removed would seem to be more promising, supported by the significantly lower value of the resulting velocity dispersion, at present we choose to take as our basic estimate of turnaround radius the average of $R_{\rm ta}$ obtained in both procedures; this gives[3]

$$R_{\rm ta} = (1.0 \pm 0.2) \text{ Mpc} . \qquad (9)$$

[3]The error estimate has been slightly biased towards a larger value of R to make the errors symmetric.

Using equations (2) we can relate the mass inside the turnaround sphere to the turnaround radius as

$$M_{\rm ta} = \frac{\pi^2 R^3}{8Gt^2} = 2.74 \times 10^{12} M_\odot \frac{R^3}{t_{10}^2} , \qquad (10)$$

where R is in Mpc and $t_{10} = t/10$ Gyr. Using Eq. (9) and accounting for the propagation of errors, we obtain $M_{\rm ta} = (3.1 \pm 1.6) \times t_{10}^{-2}\, 10^{12} M_\odot$. Taking 7/17 of this to be the Milky Way fraction, we find $M_{\rm ta}(MW) = (1.3 \pm 0.7) \times t_{10}^{-2}\, 10^{12} M_\odot$. The mass that is just outside of the first caustic should be even smaller. To find this latter mass in the $\epsilon = 1$, $\Omega_0 = 1$ model, these numbers should be multiplied by 0.7, giving

$$M_1(MW) = (0.88 \pm 0.47) \times t_{10}^{-2} \times 10^{12} M_\odot . \qquad (11)$$

We adopt these as our basic estimates of the mass of the Local Group and of the Milky Way. The further discussion in subsequent §4.2 and §4.3, is mainly for comparison.

4.2. Direct weighing of the LG using tracers of infall near the turnaround sphere.

Among those galaxies near the turnaround sphere, the galaxies IC 1613, WLM, DDO 210 and DDO 216, are closest relative to our best fit infall trajectory (see Figs. 2. and A1). On the other hand, N6822 and M31 appear to be outliers. It is, therefore, interesting to analyse IC 1613, WLM, DDO 210 and DDO 216 separately,[4] using Eqs. (4) to "weigh" the Local Group directly, without any assumptions about the shape of the initial inhomegeneity or the cosmological model. The unknown cosmological parameter of §4.1, the Hubble constant h, is replaced here by the cosmic time, t. Since the relation $h = h(t)$ is model dependent and unknown at present, this "direct weighing" may be of some interest.

We plot the total mass interior to the tracer galaxies versus cosmic time in Figure 4. We warn the consumer that conclusions derived from analysis of only a handful of galaxies should be taken cautiously. Although Mateo (1998) estimates typical distance errors in the 5 – 10% range, some galaxies in his sample have had their distance estimates vary by a factor of two. To illustrate the effect of errors in the distance estimates, we draw with

[4]Phoenix and IC 10 are closer to one of the dominant galaxies than to the center of mass (see Tables I and II), therefore we analyse them with the assumption of infall to one of the large galaxies; see below.

dotted lines in Figure 4, a ±10% error "corridor" around IC1613.

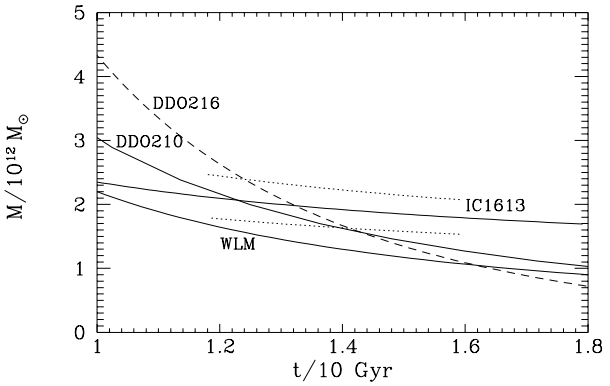

Fig. 4.— Total mass interior to a tracer galaxy versus the age of the Universe (dashed and solid curves). The dotted curves represent the ±10% error "corridor" around IC1613.

IC 1613 is probably too close for the spherical infall model to be reliable. In contrast, DDO 216 is outside the turnaround surface and is therefore still expanding with the Universe; for this reason we plot this galaxy with a dashed line in Figure 4. The best tracer galaxies could be WLM and DDO 210. DDO 210 is very close to the turnaround surface but is already inside it. We find $M(DDO210) = 3.0 \times t_{10}^{-2}\, 10^{12} M_\odot$, in good agreement with the Local Group mass estimate from Eq. (10). It appears that WLM may have fallen in even earlier, providing an even stronger constraint on the mass within the first caustic. If we adopt 10 Gyr as a lower bound for the age of the Universe, we infer (see Fig. 4) $M(0.8\,\mathrm{Mpc}) < 2.2 \times 10^{12} M_\odot$. For the total mass associated with the Milky Way we have to take 7/17 of this value, leaving the rest for M31; this gives $M_{\rm MW} \lesssim 0.9 \times 10^{12} M_\odot$. This is in agreement with our best fit estimate for the Milky Way fraction of the mass inside the first caustic (Eq. 11). [We recall that since $R_{\rm ta} \sim 1$ Mpc, the radius of the first caustic $R_1 \sim 0.37 R_{\rm ta} \sim 0.4$ Mpc and consequently WLM is outside the first caustic, although not very far from it.] Note that since the MW – M31 distance is larger than twice the radius of the first caustic, there has been no mixing between material that infalls to the Milky Way and that which infalls to M31.

Since DDO 216 is the galaxy farthest away from the center of mass, (see Table I), the total mass interior to its orbit should be the largest. However, contrary to this expectation, the dashed line on Figure 4 falls below the solid lines for $t > 13 - 16$ Gyr. This should not occur in the absence of observational errors (but, note the effect of 10% errors on the IC 1613 curve), provided that spherical infall is an adequate approximation. If so, and in the absence of errors, we could derive an upper bound to the age of the Universe, $t \lesssim 13 - 16$ Gyr. Interestingly, this suggestive bound limits the age of the Universe from above, while the more classical method, based on the ages of the oldest stars, provides bounds from below.

4.3. Infall to one of the dominant galaxies

In this subsection we present the results of an analysis of Phoenix and IC10, nearby satellite dwarf galaxies that are closer to one of the dominant galaxies than to the LG center of mass, and which lie in the hemisphere opposite the other dominant galaxy. At the same time, they are sufficiently far away to be outside the first caustic. The approximation of direct infall to the closest dominant galaxy might not be unreasonable for these dwarfs. The relevant parameters are listed in Table 2.

We have assumed that Phoenix infalls to the Milky Way and that IC10 infalls to M31. The mass interior to these satellite galaxies is shown in Figure 5 along with a 10% "error corridor" for the distance estimate. Although this results in a smaller inferred mass than our best fit estimate (Eq. 11), it is within the estimated "1σ" error.

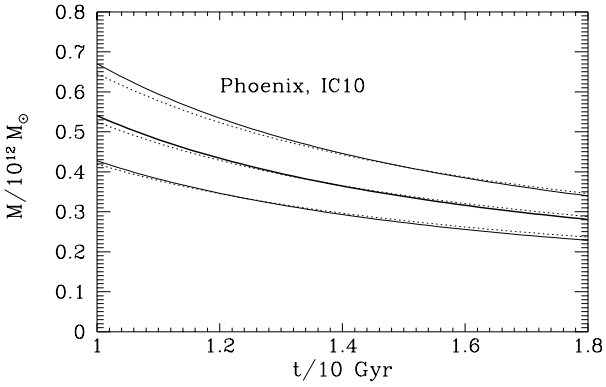

Fig. 5.— Same as Figure 4 for Phoenix (solid curves) and IC10 (dotted curves).

5. Primordial baryon fraction and Ω_0

Using equation (11) along with the MACHO results and the standard formulae for the propagation of errors we obtain a lower bound for the universal primordial baryon fraction $f_{\rm B} \gtrsim M_{\rm B}(50\ \mathrm{kpc})/M_{\rm MW} = 0.29^{+0.18}_{-0.15}\, t_{10}^2$.

This can be rewritten as

$$\Omega_{\rm B} \gtrsim 0.29^{+0.18}_{-0.15}\, t_{10}^2\, \Omega_0\,. \qquad (12)$$

Introducing the baryon-to-photon ratio $\eta = n_{\rm B}/n_\gamma$ so that $\Omega_{\rm B}h^2 = \eta_{10}/273$, where $\eta_{10} \equiv \eta/10^{-10}$, we may rewrite this equation to derive an upper bound on the total matter density, $\Omega_0 h^2 t_{10}^2 \lesssim 3.66 \times 10^{-3}\eta_{10}/f_B$. In the absence of a cosmological constant the age and Hubble parameter are related by

$$t_0 H_0 = \int_0^1 \left(1 - \Omega_0 + \Omega_0 x^{-1}\right)^{-1/2} dx, \qquad (13)$$

where $H_0^{-1} = 9.78h^{-1}$ Gyr, so that

$$\Omega_0\,(H_0 t_0)^2 \lesssim 0.020^{+0.010}_{-0.013}\,\eta_{10}\,. \qquad (14)$$

Similarly, t_0H_0 can be found as a function of Ω_0 for any given value of $\lambda_0 \equiv \Lambda/3H_0^2$. The left-hand side of equation (14) is plotted versus Ω_0 in Figure 6 for two cases, $\lambda_0 = 0$ and $\Omega_0 + \lambda_0 = 1$.

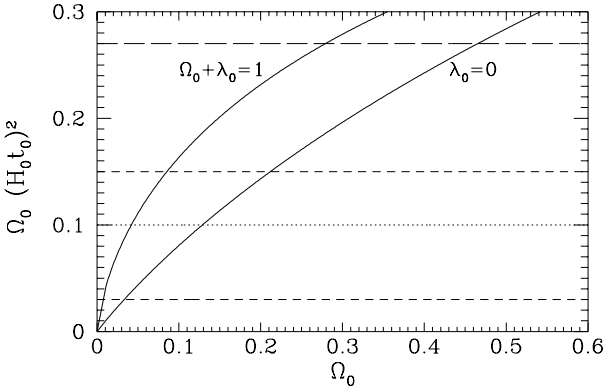

Fig. 6.— $\Omega_0(H_0t_0)^2$ versus Ω_0 (solid curves) along with our bound, Eq. (14). The dotted and dashed lines are for $\eta_{10} = 5.1 \pm 0.3$ respectively, while the long-dashed line is for the upper bound in Eq. (14) and $\eta_{10} < 9.0$.

Using SBBN to bound the right-hand side of Eq. (14), we may adopt for the nucleon-to-photon ratio the Burles & Tytler (1998) deuterium-driven estimate $\eta_{10} = 5.1 \pm 0.3$. From Figure 6 this leads to the bound, $\Omega_0 = 0.13^{+0.08}_{-0.10}$ for $\lambda_0 = 0$, or $\Omega_0 = 0.04^{+0.04}_{-0.03}$ for $\Omega_0 + \lambda_0 = 1$. As a conservative upper bound we may adopt $\Omega_0 \lesssim 0.2$. Note that, for an extreme upper bound to the nucleon-to-photon ratio derived from the lithium abundance alone (Pinsonneault et al. 1997), $\eta_{10} < 9.0$, we constrain $\Omega_0 < 0.47$ for $\lambda_0 = 0$ and $\Omega_0 < 0.28$ for $\Omega_0 + \lambda_0 = 1$ (see Figure 6). Note, however, that if the vacuum energy is cosmologically relevant, the equations of motion near the turnaround radius will be modified *independent* of the value of R. Therefore, in this case Eq. (10) is modified and, correspondingly, so too will be our bounds for the baryon fraction. However, the effect of a cosmological constant is to *decrease* $M_{\rm ta}$ at a given R and t (i.e. to *increase* f_B). Therefore, our bounds quoted here are conservative for the case of non-zero vacuum energy.

This preference for a low value of Ω_0 was already noted in Peebles et al. (1989) and Peebles (1995, 1996) based on the motions of the LG galaxies, and is consistent with recent observations on larger scales (see e.g. Bahcall et al. 1995; Kashlinsky 1998; Steigman, Hata & Felten 1997; Willick et al. 1997; Perlmutter et al. 1998).

It is interesting to compare our constraint on the universal baryon fraction, $f_B \gtrsim 0.14\ t_{10}^2$, with the baryon fraction derived from X-ray clusters, $f_B\, h^{3/2} = (1.0 \pm 0.1)(1 + h^{3/2}/5.5)/15$ (Steigman, Hata & Felten 1997; Evrard 1997). For $t_{10} \gtrsim 1$, both constraints are shown in Figure 7. Although there is reasonable agreement for $t_0 = 10$ Gyr, larger ages provide a hint of a discrepancy. Such disagreement may point towards more dark baryons in clusters (e.g., intergalactic MACHOs (Gould 1995)) than is revealed by the X-rays, or fewer LG baryons (non-baryonic halo dark matter).

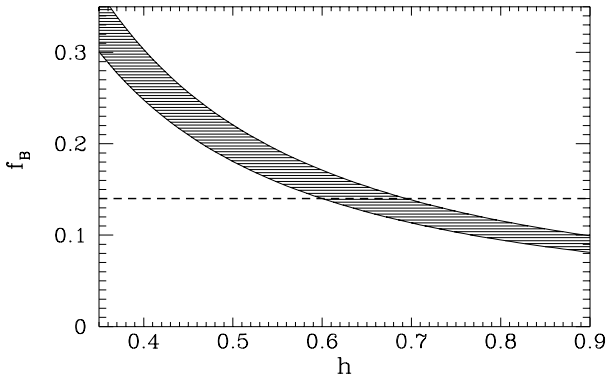

Fig. 7.— The baryon fraction – Hubble parameter plane. The crosshatched region shows the estimate of the baryon fraction derived from X-ray clusters. The dashed line is our LG constraint, $f_B > 0.14$ (for $t_0 > 10$ Gyr).

Alternatively, we may use our MW mass estimate (eq. 11) of $M_1(MW) \approx 8.8\ t_{10}^{-2} \times 10^{11} M_\odot$, along with the X-ray cluster baryon fraction estimate of $f_B \approx 1/15h^{3/2}$, to "predict" the MW baryon mass

$$M_{\rm B}(MW) \approx 5.9\ h^{-3/2} t_{10}^{-2} \times 10^{10} M_\odot. \qquad (15)$$

For $t_0 \approx 14$ Gyr and $h \approx 0.65$ (Riess et al. 1998), this estimate suggests a MW baryon mass, $M_{\rm B}(MW) \approx 6 \times$

$10^{10} M_\odot$, considerably smaller than the MACHO value, but consistent with the MW disk mass (Fukugita, Hogan, & Peebles 1997); perhaps the bulk of the MACHO events are not caused by baryonic dark matter.

6. Conclusions

There remain several uncertainties in our LG baryon fraction estimate. One possibility which would weaken or even eliminate our constraint is if some of the observed microlensing events towards the LMC were due to an intervening satellite galaxy between us and the LMC, or due to debris in the LMC tidal tail (Zhao 1996; Zhao 1997). However, the MACHO collaboration concluded (Alcock et al. 1997b) that if the lenses were in a foreground galaxy, it must be a particularly dark galaxy; see also (Gould 1998). Moreover, the first observation of a microlensing event in the direction of the Small Magellanic Cloud (SMC) (Alcock et al. 1997c), implies an optical depth in this direction roughly equal to that in the direction of the LMC. This makes it unlikely that a dwarf galaxy or a stellar stream between us and the LMC is responsible simultaneously for the observed microlensing towards the LMC and the SMC (Alcock et al. 1997b; Gould 1998). Recently, however, Gates et al. (1997) found Galactic models which explain the current microlensing data by a dark extension of the thick disk, reducing the MACHO fraction. It is to be anticipated that as more microlensing data are accumulated, these uncertainties will be resolved.

We note that even in the absence of baryonic MACHOs there is still a limit, albeit much weaker, to $f_{\rm B}$ from LG dynamics. The mass of baryons in the disk of the Galaxy provides a lower bound to $M_{\rm B}$ which is smaller by a factor of ~ 3 than the microlensing estimate we have used (Fukugita, Hogan, & Peebles 1997). Our lower bound to $f_{\rm B}$ would be reduced by this factor while our upper bound to Ω_0 would be increased by the same factor.

In summary, if the observed microlensing events are the result of baryonic MACHOs in the Galaxy halo, then the dynamics of the LG may be used to infer a *lower* bound to the universal baryonic mass fraction: $f_{\rm B} > 0.29^{+0.18}_{-0.15}\, t_{10}^2$. If primordial nucleosynthesis is used to provide an *upper* bound to the present baryonic density, we obtain an *upper* bound to the present total mass density: $\Omega_0 \lesssim 0.2$ (with an extereme upper bound derived using nucleon-to-photon ratio based on the lithium abundance being $\Omega_0 \lesssim 0.47$).

We thank S. Colombi, J. Felten, A. Gould, Kashlinsky, P. Sikivie, and A. Stebbins for useful discussions and helpful suggestions. We reserve special thanks for our referee, Jim Peebles, for his comments and questions which led to significant revision of and, we hope, improvement on our original manuscript. This work was supported at Ohio State by DOE grant DE-AC02-76ER01545.

A. Picture of infall after the removal of subclusters of galaxies.

In the fitting of the infall in §4.1, all galaxies in the volume $r < 3$ Mpc were considered. However, galaxies which form gravitationally bound groups (or pairs) of their own, will have an additional peculiar velocity, unrelated to Local Group infall. It is expected that the velocity dispersion will be smaller in modeling the infall onto the Local Group if only relatively isolated galaxies are considered. Therefore, it is interesting to repeat the analysis of §4.1 imposing such a selection. The results of such an analysis are presented in this Appendix.

Galaxies are considered to form a group if the distance between them is smaller than $0.5\,(M/M_{\rm M31})^{1/3}$ Mpc where M is the mass of the galaxy pair and $M_{\rm M31}$ is the estimated mass of M31. Such groups were removed from the sample. Since estimates for galaxy masses were not presented in Karachentsev & Makarov (1996), we took them from Peebles (1995, 1996). We also removed a galaxy pair if the mass estimate was unavailable but the distance between the pair was smaller than 0.2 Mpc. The resulting infall diagram is shown in Fig. A8, where the scale r has been extended to 4 Mpc.

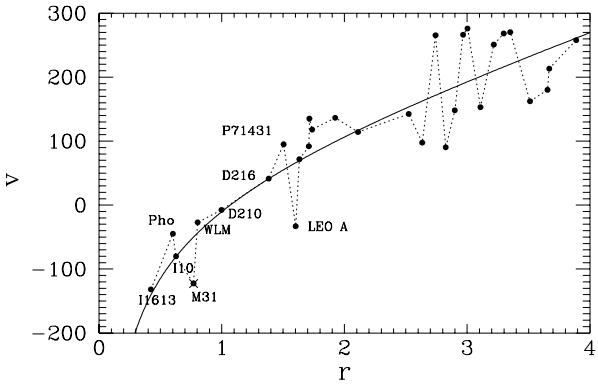

Fig. A8.— The same as Fig. 2, but after removal of close pairs of galaxies. The solid line shows the best fit infall trajectory, $R = 1.07$ Mpc, $h = 0.71$.

The velocity dispersion did become significantly smaller;

now we find $\sigma_v \approx 50$ km s^{-1}, while in §4.1 we obtained $\sigma_v \approx 70$ km s^{-1}.

In the analysis of §4.1 we had assumed that the Milky Way infalls to the common center of mass of galaxies in the volume $r < D$, while the velocity of the Galaxy with respect to those galaxies in the volume $D < r < 3$ Mpc was fitted. This allowed us to account for the possible motion of the Local Group as a whole. When we neglected the Local Group velocity, i.e., if $D = \infty$ was assumed, the quality of the fit became worse, i.e., the velocity dispersion increased. It is interesting that the corresponding effect is very small in the present situation, when galaxy subclusters are removed. Namely, by introducing the additional fitting parameters associated with the Local Group motion does reduce the scatter of the data points around the infall trajectory, while the velocity dispersion (defined as $[\sum_i^N \Delta v_i^2/(N - N_{\rm par})]^{1/2}$, where N is the number of data points and $N_{\rm par}$ is the number of fitting parameters) does not decrease. Therefore, since the analysis is consistent with the assumption of negligible Local Group motion, we do not introduce the scale D here.

Another measure of the robustness of this assumption can be obtained in the following way. The velocity of the Milky Way can be found in fits with galaxy samples of varying depth. The direction and magnitude of the resulting best fit velocity can be compared (for each value of the depth) with the original assumption of infall to the common center of mass. This trend is shown in Fig. A9 for the angular coordinates of the velocity vector, and in Fig. A10 for the amplitude of the velocity vector. (For each subsequent point in Figs. A9 and A10, the number of galaxies in the fit is increased by one.)

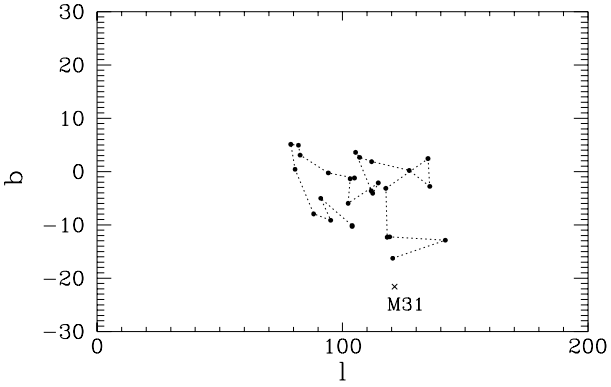

Fig. A9.— The Milky Way apex trend with respect to volumes of different depth. The Andromeda (M31) position is shown by the diagonal cross.

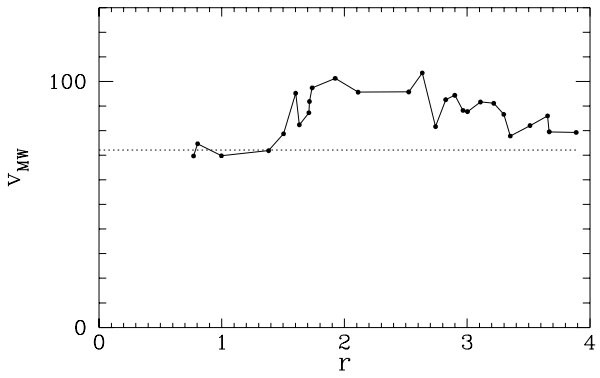

Fig. A10.— Magnitude of the Milky Way velocity towards an apex as a function of the depth of the galaxy sample. The dotted line shows our predicted velocity.

We see that with respect to nearby galaxies, the Milky Way does infall to M31 to good accuracy. Initially the direction is very close to the direction towards M31, and the magnitude is consistent with our assumption in §4.1 that at distances $r < 1.5$ Mpc, $v_{\rm MW} = v_{\rm M31}(1 + M_{\rm MW}/M_{\rm M31})^{-1}$. When the number of galaxies in the sample increases (i.e., going to larger r), the direction of the Milky Way velocity drifts away from M31, and the magnitude of the velocity vector increases for $r > 1.5$ Mpc. However, at $r \approx 4$ Mpc, both the direction and magnitude turn back and, overall, in this volume the peculair velocity of the Local Group is not significant.

A similar analysis of the trend of the MW and LG apexes was done by Karachentsev & Makarov (1996). Their assumptions were different, however. Instead of infall, Eqs. (5)-(8), they assumed pure Hubble flow for galaxies at distances $r > 1.5$ Mpc, and $v = 0$ for galaxies at distances $r < 1.5$ Mpc from the Milky Way (not from the center of mass of the Milky Way/M31 system). Also, they included all close satellites in their fit. For these reasons, our results, shown in Figs. A9 and A10, while consistent with theirs, are differing somewhat.

REFERENCES

Adams, F. C. & Laughlin, G. 1996, astro-ph/9602006

Alcock, C., et al. 1997, Ap. J. **486**, 697

Alcock, C., et al. 1997, Ap. J. **490**, L59

Alcock, C., et al. 1997, Ap. J. **491**, L11

Bahcall, N. A., Lubin, L. M., & Dorman, V. 1995, Ap. J. **447**, L81

Bertschinger, E. 1985, Ap. J. Suppl. **58**, 39

Burles, S. & Tytler, D. 1998, Ap. J. **507**, 732

Evrard, A. E. 1997, MNRAS, submitted, astro-ph/9701148

Filmore, J. A. & Goldreich, P. 1984, Ap. J. **281**, 1

Flynn, C., Gould, A., & Bahcall, J. N. 1996, Ap. J. **466**, 655

Fukugita, M., Hogan, C. J., & Peebles, P. J. E. 1997, Ap. J., submitted, astro-ph/9712020

Gates, E. I., Gyuk, G., Holder, G. P., & Turner, M. S. 1997, astro-ph/9711110

Gelb, J. M. & Bertschinger, E. 1994, Ap. J. **436**, 491

Gerhard, O. & Silk, J. 1996, Ap. J. **472**, 34

Gould, A. 1995, Ap. J. **455**, 44

Gould, A. 1998, Ap. J. **499**, 000

Gunn, J. E. & Gott, J. R. 1972, Ap. J. **176**, 1

Henriksen, R. & Widrow, L. 1995, Ap. J. **441**, 70

Kahn, F. D. & Woltjer, L. 1959, Ap. J., 130, 705

Karachentsev, I. D. & Makarov, D. A. 1996, A. J. **111**, 794

Kashlinsky, A. 1998, Ap. J. **492**, 1

Kochanek, C. 1995, astro-ph/9505068

Kolb, E. W. & Tkachev, I. I. 1994, Phys. Rev. **D50**, 769

Kulessa, A. S. & Lynden-Bell, D. 1992, Mon. Not. R. astr. Soc., **255**, 105

Mateo, M. 1998, Ann. Rev. Astron. Astrophys. **36**, 435

Peebles, P. J. E., Mellot, A. L., Holmes, M. R., & Jiang, L. R. 1989, Ap. J. **345**, 108

Peebles, P. J. E. 1995, Ap. J. **449**, 52

Peebles, P. J. E. 1996, Ap. J. **473**, 42

Perlmutter, S., et al. 1998, Nature, **391**, 51

Pinsonneault, M. H., Narayanan, V. K., Steigman, G., & Walker, T. P. 1997, astro-ph/9710035

Riess, A. G., Filipenko, A. V., Challis, P., et al. 1998, Ap. J. accepted, astroph/9805201

Ryu, D., Olive, K., & Silk, J. 1990, Ap. J. **353**, 81

Sikivie, P., Tkachev, I. I., & Yun Wang 1995, Phys. Rev. Lett. **75**, 2911

Sikivie, P., Tkachev, I. I., & Yun Wang 1997, Phys. Rev. **D56**, 1863

Steigman, G., Hata, N., & Felten, J. E. 1997, astro-ph/9708016

Steigman G. & Felten, J. E. 1995, Spa. Sci. Rev., **74**, 245

White, S. D. M., Navarro, J. F., Evrard, A. E., & Frenk, C. S. 1993, Nature **366**, 429

Willick, J. A., Strauss, M. A., Dekel, A., & Kolatt, T. 1997, Ap. J. **372**, 380

Zhao, H.-S. 1996, astro-ph/9606166

Zhao, H.-S. 1997, astro-ph/9703097

This 2-column preprint was prepared with the AAS LaTeX macros v4.0.

Table 1: The sample of Local Group galaxies. l and b are galactic coordinates; r_g and v_g are galactocentric distance (Mpc) and velocity (km/s); r (Mpc) and v (km/s) are the distance and velocity with respect to the center of mass of the Milky Way/M31 system.

	Name	l	b	r_g	v_g	r	v
0	M31	121.2	-21.6	0.77	-123		
1	IC1613	130	-60.6	0.66	-152	0.425	-130
2	Phoenix	272	-69	0.42	-33.3	0.592	-44.2
3	IC10	119	-3.3	1.04	-146	0.638	-81.9
4	N6822	25.3	-18.4	0.52	43.4	0.673	59.8
5	Sagitt	21.1	-16.3	0.57	8.11	0.738	5.46
6	WLM	75.7	-73.6	0.95	-62.6	0.804	-28.1
7	DDO210	34.1	-31.4	1	-23.4	0.995	-7.94
8	N55	333	-75.7	1.34	94.2	1.34	112
9	DDO216	94.8	-43.6	1.75	-21.1	1.39	39.5

Table 2: Same as in Table I, except now r and v are the distances and velocities with respect to the center of the Milky Way for Phoenix, and with respect to the center of M31 for IC10.

Name	l	b	r_g	v_g	r	v
Phoenix	272.2	-69.0	0.42	-33	0.42	-33
IC10	119.0	-3.3	1.04	-146	0.39	-38